


## Article

# Effects of Building Height on the Sound Transmission in Cross-Laminated Timber Buildings—Vibration Reduction Index

Erik Nilsson <sup>1,\*</sup> , Sylvain Ménard <sup>1</sup>, Delphine Bard <sup>2</sup> and Klas Hagberg <sup>3</sup>

<sup>1</sup> Department of Applied Sciences, University of Québec at Chicoutimi, Chicoutimi, QC G7H 2B1, Canada; sylvain\_menard@uqac.ca

<sup>2</sup> Department of Physics and Astronomy, Katholieke Universiteit Leuven, 3000 Leuven, Belgium; delphine.bardhagberg@kuleuven.be

<sup>3</sup> Department of Civil, Environmental and Natural Resources Engineering, Luleå University of Technology, 97187 Luleå, Sweden; klas.hagberg@ltu.se

\* Correspondence: erik.nilsson1@uqac.ca

**Abstract:** High-rise wooden buildings are increasing in popularity, and they typically include cross-laminated timber in the structure. Taller buildings result in higher loads on the junctions lower down in the building, which are suggested in the literature to negatively affect the sound insulation. This study involved measurement of the vibration reduction index in four different CLT buildings, varying in height and junction details. A total of 12 junctions were measured at both high and low levels in the buildings. Among these, 10 junctions had resilient interlayers with different stiffnesses dependent on the designed quasi-permanent load, while 2 junctions lacked resilient interlayers. The results indicated that the vibration reduction index decreases lower down in the building mainly for the *Wall–Wall* path. The findings were consistent for all measured junctions above 400 Hz for the *Wall–Wall* path and for the majority of the measurements of the remaining frequency range, 400 Hz and below. The observed difference in the vibration reduction index could significantly impact the final result if a high-rise building has several flanking paths that affect the sound insulation between two apartments, and this needs to be considered during the design phase. Similar effects were shown for buildings both with and without resilient interlayers in the junctions.

**Keywords:** vibration reduction index; building height; cross-laminated timber; building acoustics; sound insulation



**Citation:** Nilsson, E.; Ménard, S.; Bard, D.; Hagberg, K. Effects of Building Height on the Sound Transmission in Cross-Laminated Timber Buildings—Vibration Reduction Index. *Buildings* **2023**, *13*, 2943. <https://doi.org/10.3390/buildings13122943>

Academic Editors: Chiara Scrosati and Maria Machimbarrena

Received: 27 October 2023

Revised: 22 November 2023

Accepted: 23 November 2023

Published: 25 November 2023



**Copyright:** © 2023 by the authors. Licensee MDPI, Basel, Switzerland. This article is an open access article distributed under the terms and conditions of the Creative Commons Attribution (CC BY) license (<https://creativecommons.org/licenses/by/4.0/>).

## 1. Introduction

Wooden buildings are increasing in popularity and usage for various constructions, including multi-family houses, schools, and offices. Moreover, the maximum building height is gradually growing with more stories, which increases the load lower down in the building. Cross-laminated timber (CLT) is typically used in some parts of the construction of high-rise wooden buildings. CLT is built up from several layers of stacked lumber boards that are glued together in a crosswise pattern. Generally, the crosswise pattern is 90 degrees, a minimum of three glued layers are used, and the CLT elements consist of an odd number of layers. Due to the crosswise pattern and laminating process, improved dimensional stability is provided for the elements, and CLT has high strength and stiffness properties [1]. While various papers on wind, fire, and seismic performance exist for high-rise wood buildings [2–17], few investigate the acoustic factors. Previous research on acoustics in wood has mainly focused on sound transmission through single elements in a laboratory and the sound transmission in finished smaller buildings or mockups.

Several laboratories measured the performance of CLT elements with and without additional layers, including Refs. [18–25]. Vardaxis et al. [26] measured various configurations of CLT slabs, focusing on layers of wet and dry solutions above the CLT. Sabourin and McCartney [27] measured the sound insulation properties of CLT elements for floors

and walls with different thicknesses and additional linings. Loriggiola et al. [28] measured several configurations of CLT walls with frames and panels. Hongisto et al. [29] measured many wooden and concrete constructions, including CLT floors with additional layers. Moreover, some articles, including Refs. [30–36], focused on theoretical estimations and evaluations based on measurements to predict the sound insulation properties of CLT elements. Lin et al. [37] compared several calculation methods with the measurement results of CLT walls combined with frames and panels. Bader Eddin et al. [38] used an artificial neural network approach to predict the sound insulation properties of different lightweight floors based on 252 standardized laboratory measurements with good accuracy. Furthermore, sound radiation models and finite element methods were developed in a few papers [39–43] for CLT plates, which are used to predict sound insulation.

In the literature, several authors collected and measured the vibration reduction index of CLT elements, including Refs. [44–49]. Schoenwald et al. [50] presented vibration reduction index measurements of CLT elements via different connection methods that are used to predict the flanking sound transmission. Pérez and Fuente [51] measured the velocity level difference in a CLT mock-up building where, amongst other combinations, different resilient materials were used. Additionally, a more extensive mock-up test of several sound parameters, including the vibration reduction index, was conducted in the ADIVBois Acoustic Mockup [52].

A large set of measurements have been collected by various authors in the literature described above. Moreover, some researchers have observed whether the load on junctions affects the sound transmission. Ref. [50] found that the load on a junction affected the flanking sound transmission in a laboratory, but only on the initial loading of the first simulated story; further loading after that had no effect. Morandi et al. [53] expected to see a difference when adding a load on a CLT slab during measurements of the vibration reduction index in a laboratory. Conversely, they found no significant difference when a load was added, which they argue could have been caused by the construction process. Mecking et al. [54] found that an extra load marginally lowered the vibration reduction index of an L-junction. Crispin et al. [55] showed that an increasing load results in a higher dynamic stiffness of the joint and a lower global vibration reduction index for two concrete elements connected with a flexible interlayer of natural rubber. The measurements from Refs. [50,53,54] were on CLT elements from laboratories, where a field situation could be simulated. In other papers, field measurements in finished buildings were evaluated, and it was suggested that the load affects the sound transmission between apartments. Ref. [56] found that the load could have a negative effect on the flanking sound transmission in a lightweight timber construction. However, the authors suggested that this is caused by a mismatch between the load and stiffness of the resilient interlayers. Ref. [57] found that the impact sound insulation was worse lower down in the building, which they argue is due to less elasticity in the lower junctions because of the higher constraints being applied. Hörnmark [58] measured the vibration reduction index in a finished building and found that increasing the load negatively affects the vibration reduction index. However, measurements were performed with a transient method, and the vibration levels were not simultaneously recorded, which contradicts the recommendations in ISO 10848-1 [59].

Some of the previously mentioned studies [50,53–58] either measured the vibration reduction index in a laboratory or in the field, and few junctions and combinations were investigated in each paper. Moreover, only a few papers described in numbers or curves how significant the influence of the building height is, while others mainly commented on whether it has an effect. There is a need to thoroughly investigate whether the difference in building height affects the sound transmission between stories in the field and how significant the effect is. In a recent study by Nilsson et al. [60], the authors performed 58 airborne sound insulation measurements over several stories in four buildings with different building systems and junction details. The results showed that the airborne sound insulation decreases lower down in the buildings. Moreover, Ref. [60] found that the airborne sound insulation decreases at a mean value of 0.5 dB per story over the frequency

range. For a six-story difference, a 3 dB decrease in airborne sound insulation is, therefore, expected. The findings in Ref. [60] can be used for an overall estimation but strongly depend on the presence of the flanking sound transmission. Additionally, the study did not describe how the impact sound insulation is affected. For more precise estimations, measurements of the  $K_{ij}$  in several buildings are needed to determine the effect of the flanking sound transmission.

In an attempt to further investigate how the load might affect the sound insulation in finished buildings, vibration reduction index measurements in real buildings are required, as also highlighted in Ref. [60]. The purpose of this paper is to present findings from measurements and evaluations of the vibration reduction index of several CLT buildings with different junction details at different stories. The goal is to find correlations between the difference in  $K_{ij}$  and the load or the number of stories that can be used in predictions.

## 2. Vibration Reduction Index and Measurement Method

The vibration reduction index,  $K_{ij}$ , was measured on 12 junctions in four different building projects made with cross-laminated timber. The junctions were categorized in pairs (six pairs in total), where one junction pair was measured at a low level and a high level in a building (see Figure 1). The junctions within each junction pair are at the same location in a plane view with the same boundary conditions. Thus, the only main difference within the same junction pair is the load on the junction, with a few exceptions described further down for each building project.

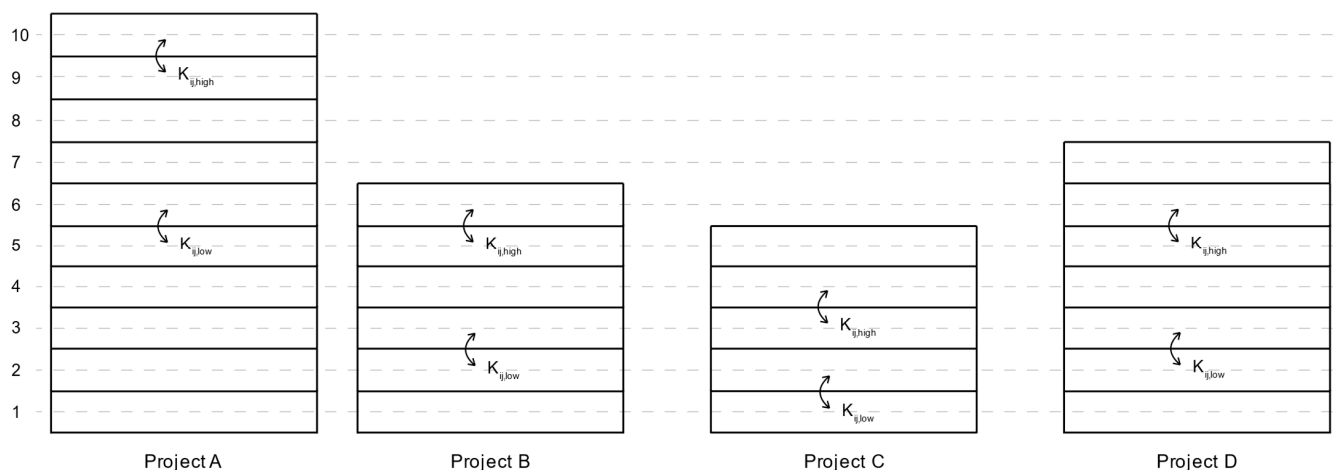


**Figure 1.** Overview of the number of stories for each project and where measurements took place at high and low stories.

The vibration reduction index,  $K_{ij}$ , was measured based on the standard ISO 10848-1 [59] and was calculated according to Equation (1):

$$K_{ij} = \overline{D_{v,ij}} + 10 \log_{10} \left( \frac{l_{ij}}{\sqrt{a_i a_j}} \right), \quad (1)$$

where  $\overline{D_{v,ij}}$  is the direction-averaged velocity level difference,  $l_{ij}$  is the junction length, and  $a_i$  and  $a_j$  are the equivalent junction lengths of the elements. The standard [59] was developed for laboratory measurements, and no measurement standard exists for the field. However, similar principles can be applied to field situations with some caution. For example, in a field situation, the operator should take note of potential flanking paths that are not first-order flanking paths. Here, first-order flanking paths are defined as paths including one junction, one source surface, and one receiving surface. ISO 10848-1 [59] describes two different measurement methods, either a transient or a steady-state method. Indeed, excitation with a steady-state method (like a shaker) is more reliable than a transient method (like a hammer), as shown in the literature [61,62]. Moreover, measurement with a

shaker is the preferred method, but an impact hammer can be used as long as simultaneous measurements on the sending and receiving elements are performed according to the standard [59]. However, it is not reasonable to bring a shaker to field measurements due to the weight of the device, handling it on-site without access to elevators, and the limited time available because of ongoing building work. Furthermore, Ref. [46] found no significant difference between measurement methods with a hammer or a shaker for CLT elements. To measure the direction-averaged velocity level difference, the velocity level difference between elements  $i$  and  $j$  ( $D_{v,ij}$ ) and between elements  $j$  and  $i$  ( $D_{v,ji}$ ) is measured. Then,  $\overline{D_{v,ij}}$  is calculated according to Equation (2):

$$\overline{D_{v,ij}} = \frac{1}{2}(D_{v,ij} + D_{v,ji}). \quad (2)$$

The velocity level difference was measured with accelerometers attached to the surface, and seven to nine accelerometers were used in total, depending on the size of the CLT plates. The measurement equipment consisted of accelerometers of type 4507 B 004 from Brüel & Kjær (Virum, Denmark), two LAN-XI of type 3050-A-060 from Brüel & Kjær, and an impact hammer of type 8210 also from Brüel & Kjær. The accelerometers were calibrated with a vibration calibrator of type VC20 from Metra (MMF) (Radebeul, Germany), and the software BK Connect (mainly version 26.0.0.241) from Brüel & Kjær was used to record, process, and analyze the data. The impact hammer is a part of the transient method, and it is shown in Figure 2a. Different hardnesses (soft, medium, tough, and hard) can be used at the tip of the hammer. On-site tests showed that there is a small difference in the result among the different tips for CLT elements. This was also found in Ref. [46] but with different tips. However, it was more challenging to excite the structure with the softest tip, and the accelerometers detected some airborne sound produced by the hardest tip. Moreover, the difference in the reverberation time of a test element was negligible between the medium tip and the tough tip when struck with different strengths, as suggested in Ref. [59], to test the measurement method. Thus, either the tough or the medium tip was used in the measurements depending on the situation at the site. The same tip was always used within the same junction pair. Furthermore, since it was the difference in the vibration reduction index between stories that is of interest, and since the junction details and measurement method were the same in each junction pair, the measurement procedure was expected to have a minor impact on the test result accuracy.

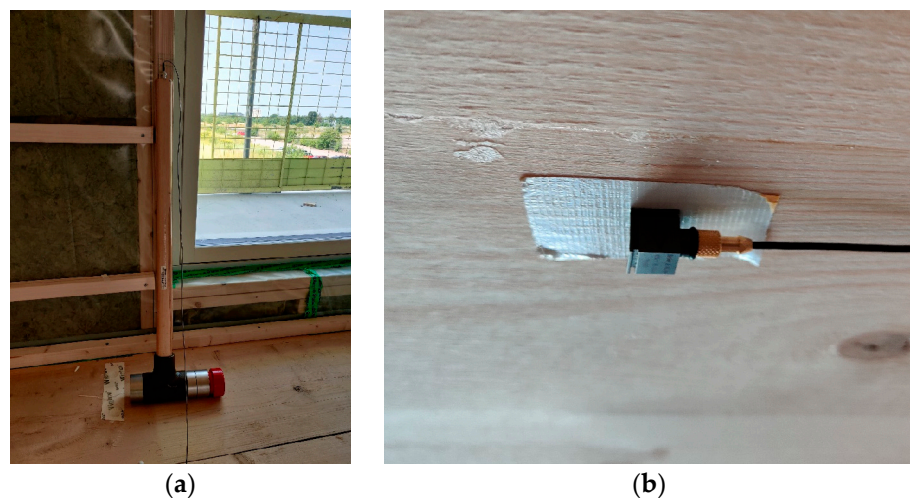


**Figure 2.** Measurement pictures of the equipment: (a) impact hammer with tough tip; (b) accelerometer mounted with double-sided tape.

For each junction, two to three excitation positions were used when measuring the difference in the average velocity level between the measured elements ( $D_{v,ij}$  and  $D_{v,ji}$ ).

The standard [59] specifies a minimum of four excitation positions for Type A elements (for example, CLT). However, this is not always suitable for field measurements because of the size of the elements and openings, even if the minimum distances are vaguely considered. In general, three excitation positions were used in the projects. However, two junctions in project A could only fit two positions, which was considered adequate, since the difference in the vibration reduction index was of interest, and since the same measurement method was applied for each junction pair. Along the two to three excitation positions, a minimum of three accelerometers were used at each element for each excitation position according to the procedure in Ref. [59]. The accelerometers were also moved around at different positions on the element, and the measurement procedure concerning minimum distances was followed based on Ref. [59]. The excitation and measurement positions were always on the same side as the flanking paths. For example, when measuring the *Ceiling–Wall* flanking path, the excitation positions and measurement positions of the ceiling/floor were performed on the ceiling instead of the floor. Furthermore, simultaneous measurements of sending and receiving elements were performed, which is strongly recommended by the standard when using the transient method. Measurement positions were recorded with accelerometers attached to the surface with double-sided tape (see Figure 2b). The standard [59] specifies that the fixing of accelerometers should be stiff in the direction normal to the surface of the elements, which is not always suitable for measurements on site, as highlighted in Ref. [63]. Thus, double-sided tape is used, and this works similarly to beeswax for frequencies up to 3150 Hz. For 3150 Hz and above, a weak fixing of the accelerometers could occur and cause errors that need to be considered [63]. Indeed, it is preferred to mount the accelerometers with screws and magnets to the CLT, instead of using beeswax or double-sided tape, to avoid weak fixing. However, this was only possible in some projects.

The structural reverberation time was measured using the same principles and procedure for the difference in average velocity levels between elements. Here, the standard specifies a minimum of three excitation positions, which is more in line with the procedure followed in the different projects. The structural reverberation times,  $T_{s,j}$  and  $T_{s,i}$ , were used to calculate the equivalent absorption lengths,  $a_j$  and  $a_i$ , according to Equation (3):

$$a_j = \frac{2.2\pi \cdot S_j}{T_{s,j} \cdot c_0 \sqrt{\frac{f}{f_{ref}}}} \quad (3)$$

where  $S_j$  is the surface area of the element measured,  $c_0$  is the speed of sound in air,  $f$  is the frequency, and  $f_{ref}$  is the reference frequency (equal to 1000 Hz [59]). The evaluation of the decay curves to determine the structural reverberation time followed the procedure in Refs. [59,64]. The evaluation range should be between 5–15 dB, according to Ref. [59]. However, shorter evaluation ranges are preferred in Ref. [65], as also highlighted in Ref. [59]. An evaluation range of 10 dB was, therefore, used, as recommended in Ref. [59].

The airborne sound produced due to impacts of the hammer was recorded by disconnecting the accelerometers from the sending and receiving elements, letting them hang in the air while the cables were attached to the elements with duct tape. The measurements in question were used to evaluate whether the airborne sound produced by the hammer, with different tips, influenced the result, while measuring the vibration reduction index.

The four building projects measured in this paper have CLT as the bearing structure for interior walls and floors. Some projects also had CLT in the facades. In this paper, the junction types (X and T) consisted of two walls and a floor. For the X-junctions, the floor was on both sides of the walls, either continuous or divided. For the T-junctions, the floor stopped in line with the two walls, with no other connections afterward.

Project A was a 10-story building with a 6 mm viscoelastic interlayer between the floor and the walls above it. The CLT elements were connected with brackets that are mounted directly onto the CLT without resilient interlayers (see Figure 3a). The measurements for project A were performed on six junctions, yielding three junction pairs: two interior

X-junction pairs and one facade T-junction pair. The difference in the number of stories between the measurements for project A was four stories for all three junction pairs. All the junctions in project A consisted of 180 mm thick CLT floor elements. All three junctions measured lower down in the building consisted of 160 mm thick CLT wall elements. For the junctions higher up in the building in project A, all three consisted of 120–140 mm thick CLT wall elements (120 mm for the upper wall elements at all three junctions, and 140 mm for the lower wall elements at all three junctions). The junctions called *Int.Wall 2* had continuous floors, while the junctions called *Int.Wall 1* had no continuous floors.

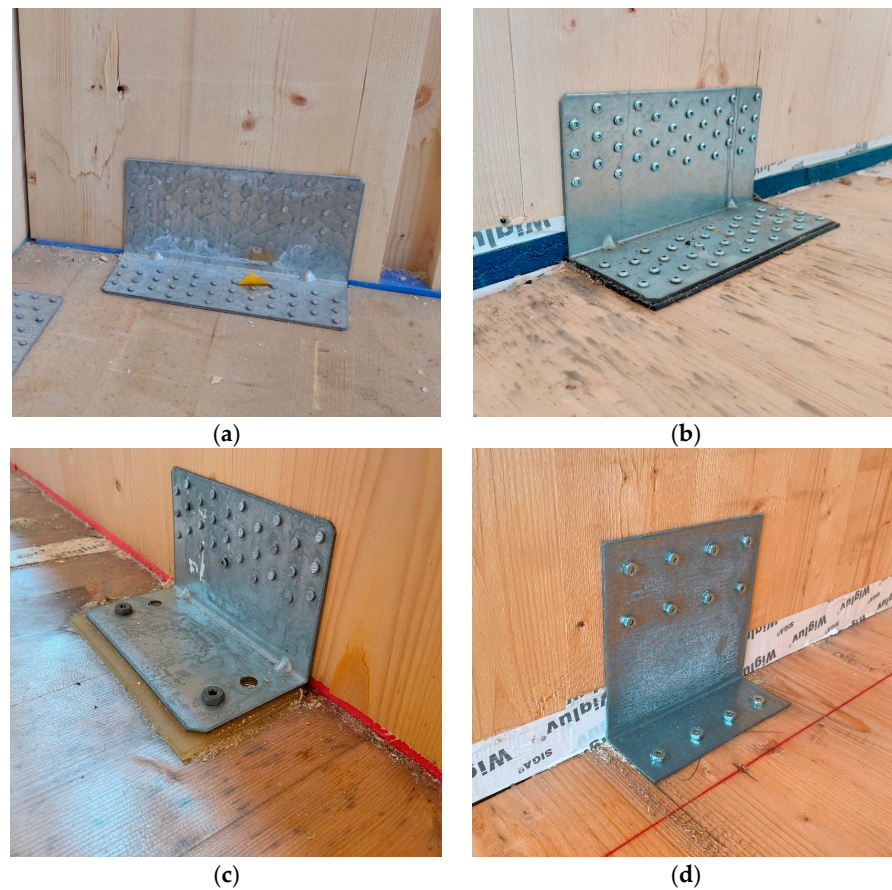


**Figure 3.** Measurement pictures of the different junction details. (a) Junction detail for project A with a 6 mm viscoelastic interlayer between CLT wall and floor and no interlayers between bracket and CLT elements. (b) Junction detail for project B with a 25 mm viscoelastic interlayer between CLT wall and floor and a thin resilient interlayer between bracket and CLT elements. (c) Junction detail for project C with a 12 mm viscoelastic interlayer between CLT wall and floor and a 6 mm resilient interlayer between bracket and CLT-elements. (d) Junction detail for project A with no interlayers in the vertical junctions.

The measurements for project B took place in a six-story building with a 25 mm viscoelastic interlayer between the floor and the walls above it. The CLT elements were connected with brackets and screws, and a thin resilient interlayer was located on the lower part of the brackets against the floor (see Figure 3b). Two X-junctions with continuous floors (one junction pair) were measured with a three-story difference. Both junctions consisted of 180 mm thick CLT floor elements and 120 mm thick CLT wall elements.

Project C was a five-story building (including the attic) with a 12 mm viscoelastic interlayer between the floor and the walls above it. The CLT elements were connected with brackets that are mounted directly onto the CLT-wall, with a 6 mm resilient interlayer between the bracket and the CLT floor (see Figure 3c). Measurements were performed

on two T-junctions, yielding one junction pair over a two-story difference. Both junctions consisted of 240 mm thick CLT floor elements and 120 mm thick CLT wall elements.

Measurements for project D took place in a seven-story building without a resilient interlayer in the vertical junctions (between floors and walls). The CLT floors and walls were connected with brackets and screws, also without a resilient interlayer (see Figure 3d). One junction pair, consisting of two interior X-junctions with a three-story difference, was measured, and the floors were not continuous for the junctions. Both junctions consisted of 250 mm thick CLT floor elements and 130 mm thick CLT wall elements.

A description of the thicknesses and the static E-modulus for the resilient interlayers that were used in the measured vertical CLT junctions is presented in Table A1.

### 3. Results

#### 3.1. Evaluation of Structural Reverberation Time

ISO 10848-1 [59] suggests that measurements with an impact hammer should be evaluated with different strengths of the hammer blow, combined with different materials on the tip. Different materials are discussed in Section 2. To evaluate the strength of the hammer blow, measurements of the reverberation time for two floors in project C are compared and displayed in Figure 4. The hammer was struck from both the ceiling and the floor. The impacts on the ceiling were lower in strength than on the floor. The result in Figure 4 indicates that there was a small difference in reverberation time between the measurements overall. A comparison was made between lines of the same type, for example, solid dark blue compared to solid light blue. Furthermore, the measurements of different floors in project C showed a small variation in reverberation time in comparison to each other.

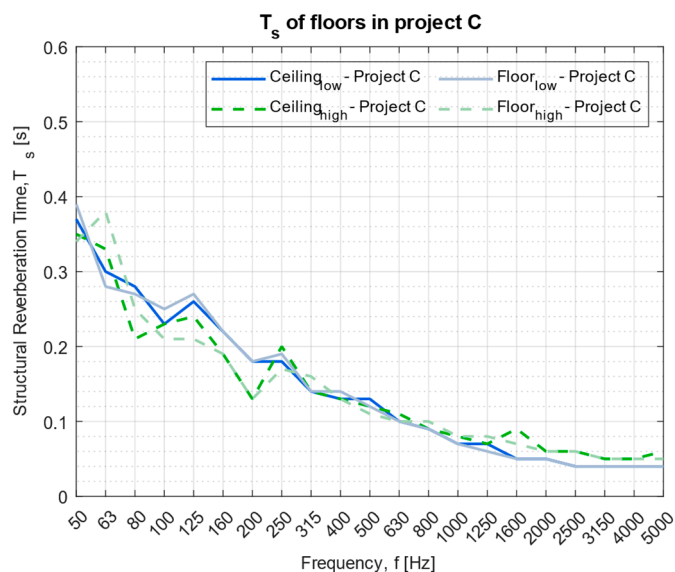


**Figure 4.** Difference in structural reverberation time of floors in project C when an impact hammer was struck from under (ceiling) and above (floor). Dashed curves represent the floor at the higher story, and solid lines represent the floor at the lower story.

#### 3.2. Vibration Reduction Index Measurements

Based on vibration reduction index measurements from four CLT projects with a total of 12 junctions consisting of 36 flanking paths, the results indicated that there is a difference in the vibration reduction index between apartments located on high stories compared to those located on low stories. In Figure 5, the difference in the vibration reduction index for the Wall–Wall path is displayed for all projects. The T-junctions (facades) are shown with dashed lines, and the X-junctions (interior walls) are displayed with solid lines. A positive difference in Figure 5 indicates that the vibration reduction index is decreasing

lower down in the building. Overall, there was a positive difference for all curves above 400 Hz. Furthermore, below 400 Hz, the curves in Figure 5 vary around 0 dB, with most of the curves also being positive. Initially, the curves have no good correlation, and one of the dashed curves is much higher than the rest. The results above 3150 Hz had a higher uncertainty due to the accelerometer mounting technique.

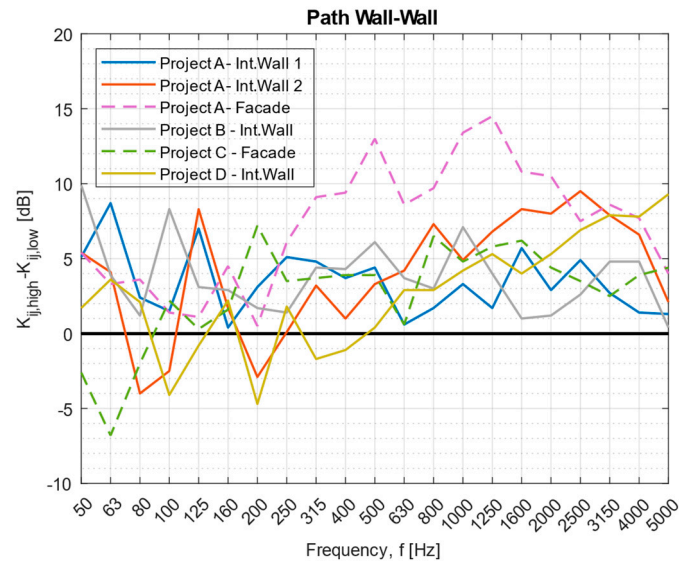


**Figure 5.** Difference in vibration reduction index for the *Wall–Wall* path between apartments situated at high and low stories for four different projects. Dashed curves represent T-junctions (facades), and solid lines represent X-junctions (interior walls).

The difference in the vibration reduction index for the *Wall–Ceiling* path is displayed for all projects in Figure 6. Similar to the result in Figure 5, the curves were mainly positive with some variations around 0 dB, indicating that the vibration reduction index was decreasing lower down in the building where the load on the junctions was higher. However, the curves were more consistent with each other, and a more apparent correlation was seen without adjustments. The results above 3150 Hz had a higher uncertainty due to the accelerometer mounting technique.

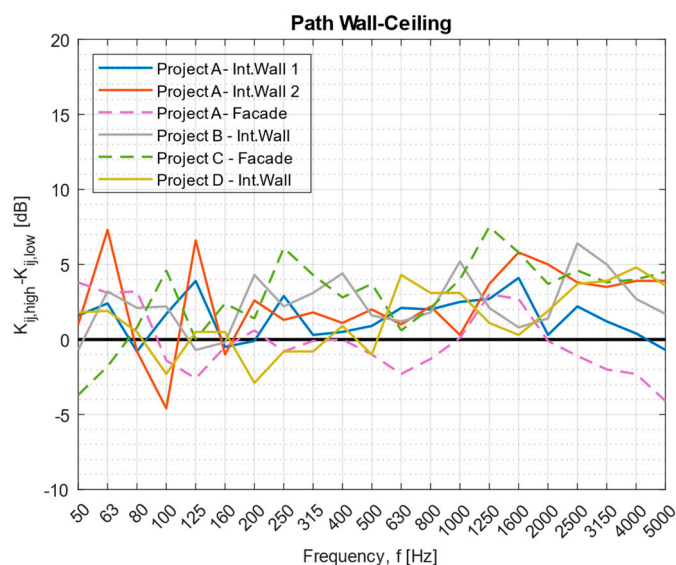


**Figure 6.** Difference in vibration reduction index for the *Wall–Ceiling* path between apartments situated at high and low stories for four different projects. Dashed curves represent T-junctions (facades), and solid lines represent X-junctions (interior walls).



Lastly, the difference in vibration reduction index for the *Wall–Floor* path is displayed for all projects in Figure 7. The same result was not found here compared to the curves shown in Figures 5 and 6. A few curves in Figure 7 vary more around 0 dB. Overall, the mean value was still positive (indicating that the vibration reduction index was decreasing lower down in the building) but not as apparent. Moreover, the curves were not consistent with each other, and no correlation was found without adjustments. Again, results above 3150 Hz had a higher uncertainty due to the accelerometer mounting technique.

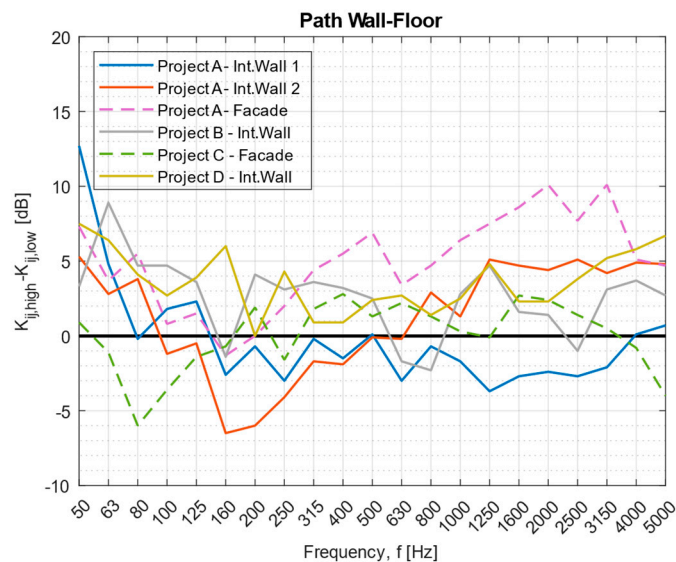


**Figure 7.** Difference in vibration reduction index for the *Wall–Floor* path between apartments situated at high and low stories for four different projects. Dashed curves represent T-junctions (facades), and solid lines represent X-junctions (interior walls).

#### 4. Discussion

The junction pairs measured for the four projects have a different number of stories between them and different loads that affect the junctions. Thus, correlations with these factors are interesting to analyze in further detail.

##### 4.1. Measurements Correlated with the Load

First, a correlation factor including the load was used to compare the results. Different load combinations could be used to find a suitable correlation factor, including combinations of the actual load when measurements took place and the quasi-permanent load combination that was used to choose the resilient interlayers in the finished buildings. However, it was only possible to obtain the load combinations for finished buildings. For these load combinations, the quasi-permanent load was relevant to use since it directly affected the choice of stiffness of the resilient interlayers in the junctions on the different stories for three of the four projects (one project had no resilient interlayers in the junctions). The load correlation factor according to Equation (4) is used:

$$\Delta K_{ij}/0.08 \cdot \log_{10} \left( (1.2\pi)^{(\Delta Load+14)} \right), \quad (4)$$

where  $\Delta Load$  is the quasi-permanent load in kN/m, and the result is displayed in Figures 8–10 for the various paths. The y-axes in Figures 8–10 are based on a reference number divided by the denominator in Equation (4), called the mean load correlation factor. This factor used the mean value of the  $\Delta Load$  from all the measurements in this article. The correlation factor in Equation (4) was first developed based on an iterative process. Later, it was adjusted so that the y-axis for both correlation methods matched (correlation with the number of stories and correlation with the load).

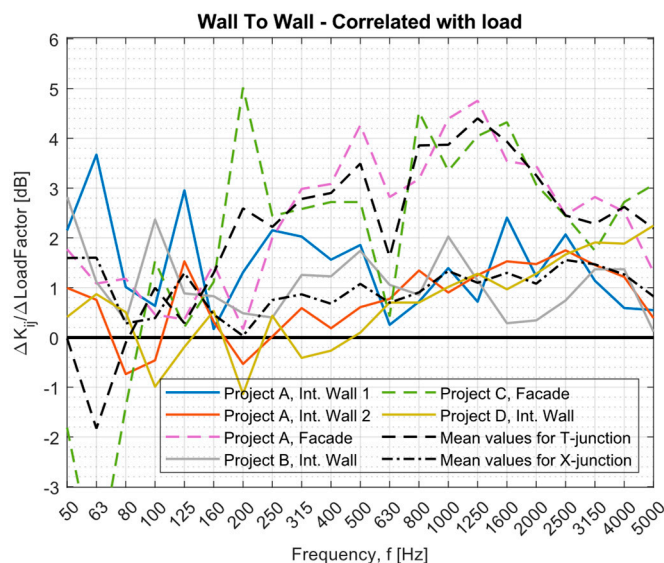


**Figure 8.** Difference in vibration reduction index for the *Wall–Wall* path, correlated with the load according to Equation (4), between apartments situated at high and low stories for four different projects. Dashed curves represent T-junctions (facades), and solid lines represent X-junctions (interior walls). Black curves represent mean value prediction curves.

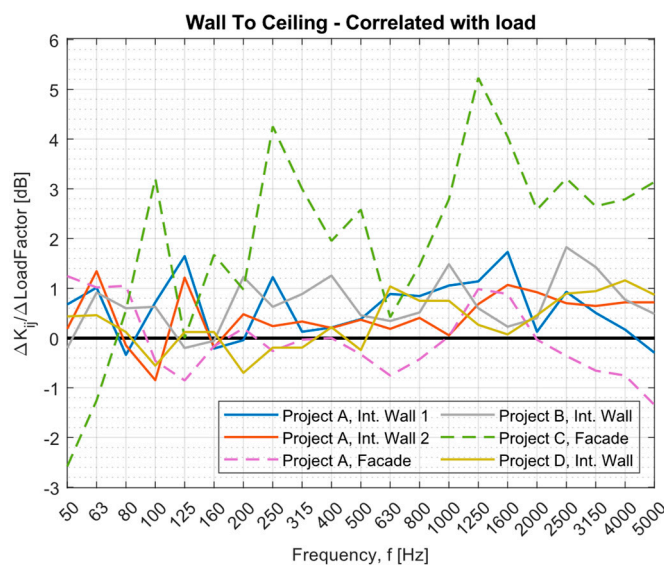


**Figure 9.** Difference in vibration reduction index for the *Wall–Ceiling* path, correlated with the load according to Equation (4), between apartments situated at high and low stories for four different projects. Dashed curves represent T-junctions (facades), and solid lines represent X-junctions (interior walls).

For the *Wall–Wall* path, mean value curves are displayed for X-junctions and T-junctions, since a correlation is found between the junction pairs and the difference between the X-junctions and T-junctions. The correlation is accurate for the T-junctions above 200 Hz, where the curves follow each other. However, for 200 Hz and below, the curves do not correlate with the load factor proposed in Equation (4). For the X-junctions, a good correlation is found for frequencies above 500 Hz. The correlation is also quite good for frequencies 500 Hz and below, but with slightly higher deviations. Overall, the correlation factor in Equation (4) results in a better correlation between the curves in Figure 8 compared to the results in Figure 5.

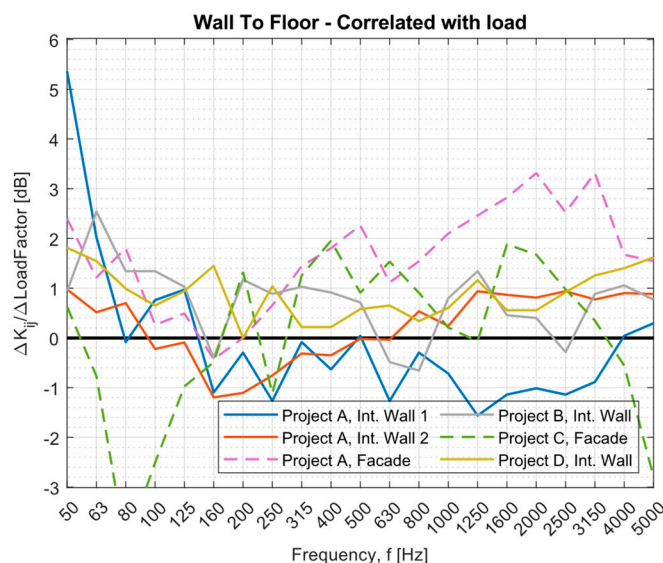


**Figure 10.** Difference in vibration reduction index for the *Wall–Floor* path, correlated with the load according to Equation (4), between apartments situated at high and low stories for four different projects. Dashed curves represent T-junctions (facades), and solid lines represent X-junctions (interior walls).

For the *Wall–Ceiling* transmission path, the correlation factor according to Equation (4) does not show a good correlation between the curves in Figure 9. Thus, the black mean value curves are not displayed in Figure 9.

For the *Wall–Floor* transmission path, the correlation factor according to Equation (4) again does not show a good correlation between the curves in Figure 10. As a result, the black mean value curves are not displayed in Figure 10 either.

The common denominator between the *Wall–Floor* and *Wall–Ceiling* paths is the floor itself, and the floor is not a vertical element in contrast to the walls. Hence, this factor could be attributed to the lack of promising results in correlation with the load for the vibration reduction index paths that include the floor. It could also explain why the correlation performs well when only vertical elements, such as walls, are considered.

It would be interesting to correlate the result with a load combination when the measurements occurred. However, the same principal loads per story are more or less affecting the junctions when the measurements take place among the different projects, since measurements are made just after the CLT elements are mounted for each project. Thus, a correlation factor with the number of stories could show similar results, if we assume a linear correlation between the stories.

#### 4.2. Measurements Correlated with the Number of Stories

As an alternative to correlating the result with the load, the difference in the number of stories within each junction pair is used according to the story correlation factor in Equation (5):

$$\Delta K_{ij} / \Delta \text{Number of stories}, \quad (5)$$

and the results are displayed in Figures 11–13. The y-axes in Figures 11–13 are based on a reference number that is divided by the denominator in Equation (5), called the mean story correlation factor. This factor uses the mean value of the  $\Delta \text{Number of stories}$  from all the measurements in this article. The same reference number is used for correlations with the load and the number of stories. A somewhat better correlation is seen with the number of stories in Figure 11 compared to the load in Figure 8 for the *Wall–Wall* path for both the T-junctions and X-junctions. This is statistically evaluated for the whole frequency range up to 3150 Hz, with both the root-mean-square error (RMSE) and the mean absolute error (MAE). Both are assessed, since the RMSE is more sensitive than the MAE to outliers [66]. However, varying results are obtained by evaluating the RMSE and

the MAE for different frequency regions (low (50–200 Hz), mid (250–1000 Hz), and high (1250–5000 Hz)) according to Hopkins [67]. The high-frequency region in this article was chosen as 1250–3150 Hz instead of 1250–5000 Hz because of a higher uncertainty in the measurement method for frequencies above 3150 Hz. The correlation with the load was found to be the best for the X-junctions at higher frequencies, while the correlation with the number of stories was found to be the best at lower frequencies for both the X- and T-junctions. The correlation with the load at higher frequencies was found to perform similarly as the correlation with the number of stories for the T-junctions. Both correlation methods performed similarly for the mid-frequency region, although the number of stories performed slightly better. The overall mean prediction values per story were calculated as 1.0 dB for the X-junctions and 1.6 dB for the T-junctions. The detailed prediction values are displayed in Figure A1, and the statistical results are shown in Figure A2.

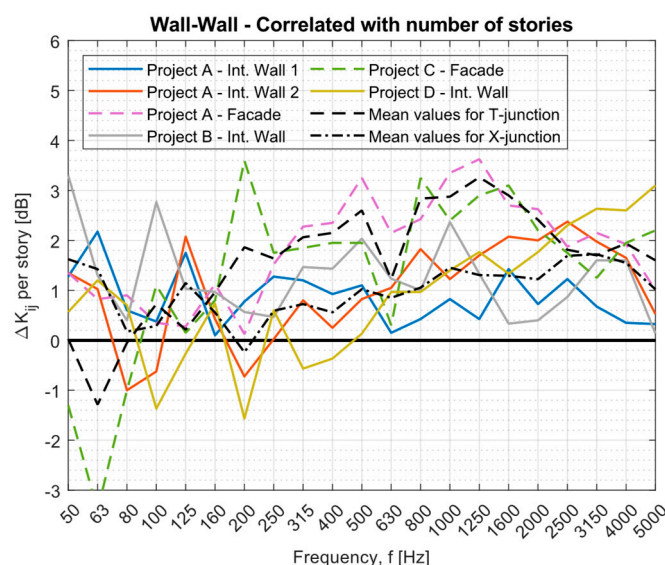


**Figure 11.** Difference in vibration reduction index for the *Wall–Wall* path, correlated with the number of stories according to Equation (5), between apartments situated at high and low stories for four different projects. Dashed curves represent T-junctions (facades), and solid lines represent X-junctions (interior walls). Black curves represent mean value prediction curves.

For the *Wall–Ceiling* transmission path, the correlation factor according to Equation (5) does not show a good correlation among the curves in Figure 12. However, the correlation factor according to Equation (5) in Figure 12 performs better than the correlation factor according to Equation (4) in Figure 9.

For the *Wall–Floor* transmission path, the same result as the *Wall–Ceiling* path, as shown above, is found in Figure 13. The correlation factor according to Equation (5) performs better in Figure 13 than the correlation factor according to Equation (4) in Figure 10, and the correlation is not good between the curves in Figure 13.

The correlation factors in Equations (4) and (5) mainly depend on the difference in load or the number of stories. They could be improved by including frequency-dependent correlations, since there could be different behaviors around, for example, the various critical frequencies of the systems. By including other parameters in Equations (4) and (5), better correlations could be achieved, specifically in the mid- and lower-frequency regions below 400 Hz, where a lower correlation is seen compared to the higher frequencies above 400 Hz. However, more vibration reduction index measurements of various junction details in CLT are needed in the field to include more parameters in the correlations.

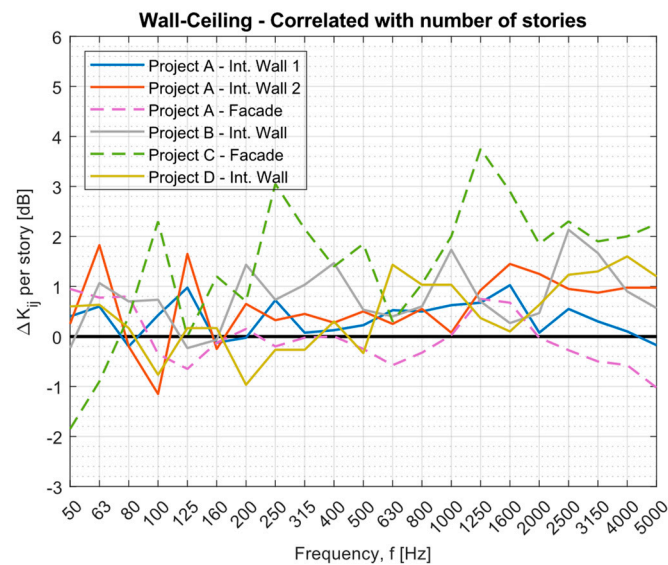


**Figure 12.** Difference in vibration reduction index for the *Wall–Ceiling* path, correlated with the number of stories according to Equation (5), between apartments situated at high and low stories for four different projects. Dashed curves represent T-junctions (facades), and solid lines represent X-junctions (interior walls).

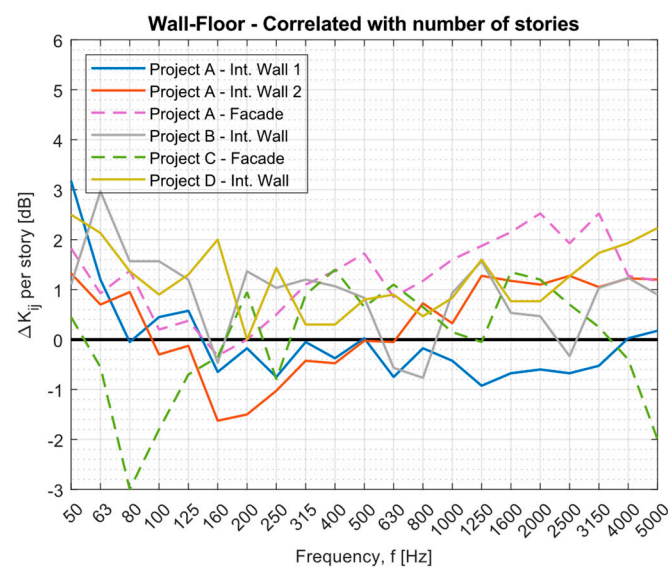


**Figure 13.** Difference in vibration reduction index for the *Wall–Floor* path, correlated with the number of stories according to Equation (5), between apartments situated at high and low stories for four different projects. Dashed curves represent T-junctions (facades), and solid lines represent X-junctions (interior walls).

#### 4.3. In-Depth Analysis

The quasi-permanent load combination is chosen as the input for the load correlation factor (Equation (4)), since that load combination is used when the resilient interlayers are dimensioned. A slightly worse correlation is observed with the load compared to the number of stories for frequencies in the mid and low regions. One possible explanation for this outcome may be the choice of resilient interlayers compared to the actual load. Even if the resilient interlayers are designed for the right load, they are chosen based on a load interval that could cover a broad load range from some manufacturers. Furthermore,  $K_{ij}$  is measured on the CLT elements while they are visible, long before the building is completed. The load is, therefore, different when measurements occur compared to the

designed load values in the finished building, including larger dead loads and live loads. With this argument, the load when measurements occur should be used instead of the designed load in a finished building. However, the load when measurements take place is not representative for the chosen stiffness of the resilient interlayers in the finished building. The relation between the load and stiffness is expected to be more relevant, since the resilient interlayers' stiffness could directly affect the vibration reduction index, as shown for some materials in Refs. [45,53]. Moreover, load combinations of just the bare CLT are only possible to be retrieved for some projects. Also, as argued at the end of Section 4.1, load combinations with only the bare CLT could have roughly the same correlation as the number of stories, if a linear correlation is assumed between the different stories.

The different stiffnesses of the resilient interlayers are chosen based on the quasi-permanent load, as previously described. Thus, stiffer resilient interlayers are chosen lower down in the building compared to the upper levels. As the literature [45,53] shows, stiffer resilient interlayers contribute to a higher vibration transmission over a junction. Therefore, it could be argued that the result obtained in this study is related to the difference in stiffness of the resilient interlayers over the number of stories. However, as shown in project D, junctions without resilient interlayers show similar results as junctions with resilient interlayers. Furthermore, a previous paper [60] that measured the airborne sound transmission in similar buildings found the same similarity as shown in this paper. While the difference in stiffness of the resilient interlayers over the number of stories might have an effect, this does not solely explain the result found in this study. Therefore, an increasing load is found to negatively affect the vibration reduction index with or without resilient interlayers in the junctions, and a higher flanking sound transmission is expected at lower levels in the buildings. The explanation, as the previous literature suggested [55], is that an increasing load yields stiffer junctions that result in a lower vibration reduction index. Hence, the load on the junctions needs to be considered with increasing stories in high-rise buildings.

The measurement results for the paths including the floor/ceiling show a slightly positive difference overall between  $K_{ij}$  at high and low stories, with a smaller  $K_{ij}$  lower down in the building. Moreover, analysis indicates that the *Wall–Wall* path yields a better result with the correlation factors than paths including the floor, compared to with no correlations. The difference in correlation performance could be caused by the fact that a floor is not affected to the same degree by the load as a vertical element, like a wall. However, the junction itself should be affected and have a result on the vibration reduction index. Furthermore, measurements of the directional average velocity level difference show that the velocity level difference varies more depending on the direction when the floor/ceiling is included, compared to the *Wall–Wall* path. For the *Wall–Wall* path, the velocity level difference is almost identical in either direction. Whether this is due to the measurement procedure or other physical parameters is uncertain at the moment and requires further investigation.

The measurements in Ref. [50] showed that the load primarily affects the vibration reduction index up to an initial load of the first story and that an additional increased load does not change the acoustical propagation properties. The measurements of the junctions in this paper described as *high* are junctions that are situated on the upper stories. Measurements also take place when the CLT elements are visible. The load is, therefore, smaller when measurements occur compared to a finished building. Thus, the result shown in this paper could be related to the same findings seen in Ref. [50]. However, the measurements in Ref. [60] were not at the highest stories, and the airborne sound insulation was measured in the finished buildings with the right load where a difference per story was found. Furthermore, a correlation between the number of stories and the load yields a good result in this paper over the frequency span for the *Wall–Wall* path and specifically for the T-junctions above 200 Hz. In contrast, the same correlation accuracy is not found for the two other paths, which could be more related to the findings in Ref. [50]. Consequently, the mean value curves, presented in Figure A1, can be used when estimating the decrease in sound insulation and the need for additional treatments lower down in the building.

However, they should be used with some caution, since they are field measurements and were only verified by one operator in four buildings. Additional measurements of the junctions in finished buildings, for each story, are needed to find more accurate estimations. This includes measurements where the difference in the number of stories is higher than four, to see if the effect is similar for even taller high-rise buildings than the ones measured in this paper.

## 5. Conclusions

The purpose of this study was to evaluate the vibration reduction index of several CLT buildings with different junction details at different stories, based on in situ measurements.

The measurements in this study indicate that the number of stories, or the load, has a negative effect on the vibration reduction index of the junctions in CLT buildings. A higher flanking sound transmission and a decrease in sound insulation are expected lower down in the building. The statement is supported by measurements from several buildings with various junction types, as shown in Figure 3. Also, the same tendency is seen for junctions without resilient interlayers. Therefore, the number of stories, or the load, is the primary factor for the building height effect, rather than the difference in the stiffness of the resilient interlayers.

The measurements were evaluated between two- and four-story differences, where individual junction pairs for the *Wall–Wall* path can differ by more than 10 dB in the vibration reduction index for specific third-octave band frequencies. In addition, the mean difference per story for the *Wall–Wall* path was calculated as 1.0 dB for the X-junctions and 1.6 dB for the T-junctions, with a decreasing vibration reduction index lower down in the building. If several flanking paths affect the sound insulation, and if the building has several stories, these factors can significantly affect the final result. Consequently, the number of stories, or the load, needs to be considered during the design phase for acoustical treatments.

**Author Contributions:** Methodology, E.N.; formal analysis, E.N.; investigation, E.N.; writing—original draft preparation, E.N.; writing—review and editing, E.N.; visualization, E.N.; review, S.M., D.B. and K.H.; supervision, S.M. and D.B. All authors have read and agreed to the published version of the manuscript.

**Funding:** This research received no external funding.

**Data Availability Statement:** The differences in the vibration reduction index presented in this study are available on request from the corresponding author. The data are not publicly available due to privacy.

**Acknowledgments:** The authors are grateful for access to the building sites and the load data provided by various construction companies, including Timratec.

**Conflicts of Interest:** The authors declare no conflict of interest.

## Appendix A

Frequency Hz	T-junction dB	X-junction dB	Frequency Hz	T-junction dB	X-junction dB
50	-0.0	1.6	50	0.0	1.6
63	-1.8	1.6	63	-1.3	1.4
80	-0.1	0.3	80	-0.0	0.2
100	1.0	0.4	100	0.7	0.3
125	0.3	1.3	125	0.2	1.1
160	1.3	0.5	160	1.0	0.6
200	2.6	0.0	200	1.9	-0.2
250	2.2	0.8	250	1.6	0.6
315	2.8	0.9	315	2.1	0.7
400	2.9	0.7	400	2.1	0.6
500	3.5	1.1	500	2.6	1.0
630	1.6	0.7	630	1.2	0.8
800	3.9	0.9	800	2.8	1.1
1000	3.9	1.3	1000	2.9	1.5
1250	4.4	1.1	1250	3.3	1.3
1600	3.9	1.3	1600	2.9	1.3
2000	3.3	1.1	2000	2.4	1.2
2500	2.5	1.6	2500	1.8	1.7
3150	2.3	1.5	3150	1.7	1.7
4000	2.6	1.3	4000	1.9	1.5
5000	2.2	0.8	5000	1.6	1.0

(a)

(b)

**Figure A1.** Detailed data for mean predicted values. (a) Data for black curves shown in Figure 8, for correlation with the load; (b) data for black curves shown in Figure 11, for correlation with the number of stories.

## Appendix B

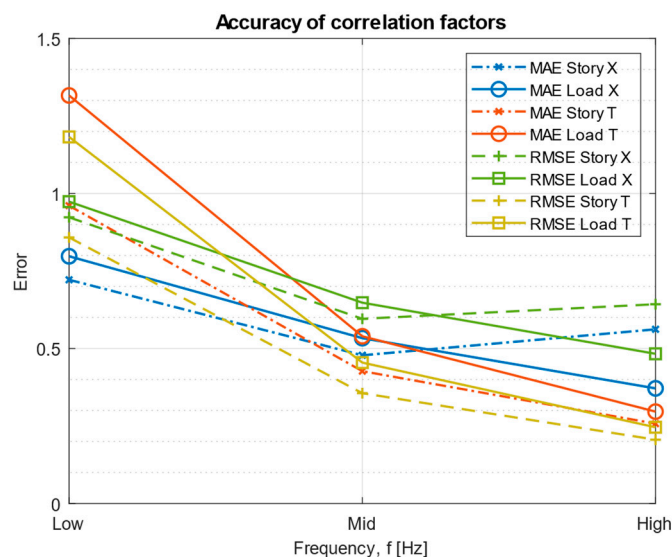


**Figure A2.** Statistical analysis of the different correlation factors with RMSE and MAE for both X-junctions and T-junctions of the Wall–Wall path.

**Table A1.** Data for the resilient interlayers used in measured vertical junctions for the different projects between CLT elements. Project A uses a mixed cellular polyether urethane; projects B and C use a mixed cellular polyurethane.

Project and Wall Type	Stories	Thickness	Static E-Modulus	Dynamic E-Modulus
Project A, int. wall 1	5–6	6 mm	1.64 N/mm <sup>2</sup> (1)	3.63 N/mm <sup>2</sup> (1)
Project A, int. wall 1	9–10	6 mm	0.453 N/mm <sup>2</sup> (1)	1.06 N/mm <sup>2</sup> (1)
Project A, int. wall 2	5–6	6 mm	8.16 N/mm <sup>2</sup> (1)	21.5 N/mm <sup>2</sup> (1)
Project A, int. wall 2	9–10	6 mm	0.931 N/mm <sup>2</sup> (1)	2.27 N/mm <sup>2</sup> (1)
Project A, facade	5–6	6 mm	4.57 N/mm <sup>2</sup> (1)	10.4 N/mm <sup>2</sup> (1)
Project A, facade	9–10	6 mm	0.861 N/mm <sup>2</sup> (1)	1.86 N/mm <sup>2</sup> (1)
Project B, int. wall	2–3	25 mm	7.23 N/mm <sup>2</sup> (2)	11.08 N/mm <sup>2</sup> (1)
Project B, int. wall	5–6	25 mm	0.83 N/mm <sup>2</sup> (2)	1.52 N/mm <sup>2</sup> (1)
Project C, facade	1–2	12 mm	3.36 N/mm <sup>2</sup> (2)	5.42 N/mm <sup>2</sup> (1)
Project C, facade	3–4	12 mm	0.83 N/mm <sup>2</sup> (2)	1.52 N/mm <sup>2</sup> (1)
Project D, int. wall	2–3	- (3)	- (3)	- (3)
Project D, int. wall	5–6	- (3)	- (3)	- (3)

(1) Test method according to DIN 53513. (2) Calculated by the manufacturer as the first derivative of the static load deflection curve. (3) No resilient interlayers were used in the vertical junctions.

## References

1. FPInnovations. *Canadian CLT Handbook*; Karacabeyli, E., Gagnon, S., Eds.; FPInnovations: Pointe-Claire, QC, Canada, 2019; Volume 1.
2. Barber, D. Fire Safety of Mass timber Buildings with CLT in USA. *Wood Fiber Sci.* **2018**, *50*, 83–95. [CrossRef]
3. Barber, D. Tall Timber Buildings: What's Next in Fire Safety? *Fire Technol.* **2015**, *51*, 1279–1284. [CrossRef]
4. Barber, D.; Rackauskaite, E.; Christensen, E.; Schulz, J. Exposed Mass Timber in High-Rise Structures: A Practical Discussion of a Complex Fire Problem. *CTBUH J.* **2022**, *1*, 32–39.
5. Gernay, T.; Ni, S. *Timber High Rise Buildings and Fire Safety*; World Steel Association: Brussels, Belgium, 2020; p. 119.
6. Gorska, C.; Hidalgo, J.P.; Torero, J.L. Fire dynamics in mass timber compartments. *Fire Saf. J.* **2021**, *120*, 103098. [CrossRef]
7. Hayajneh, S.M.; Naser, J. Fire Spread in Multi-Storey Timber Building, a CFD Study. *Fluids* **2023**, *8*, 140. [CrossRef]
8. Lazzarini, E.; Frison, G.; Truttali, D.; Marchi, L.; Scotta, R. Comfort assessment of high-rise timber buildings exposed to wind-induced vibrations. *Struct. Des. Tall Spec. Build.* **2021**, *30*, e1882. [CrossRef]
9. Li, Z.; Tsavdaridis, K.D. Design for Seismic Resilient Cross Laminated Timber (CLT) Structures: A Review of Research, Novel Connections, Challenges and Opportunities. *Buildings* **2023**, *13*, 505. [CrossRef]



10. Xing, Z.; Wang, Y.; Zhang, J.; Ma, H. Comparative study on fire resistance and zero strength layer thickness of CLT floor under natural fire and standard fire. *Constr. Build. Mater.* **2021**, *302*, 124368. [[CrossRef](#)]
11. Pan, Y.; Tannert, T.; Kaushik, K.; Xiong, H.; Ventura, C.E. Seismic performance of a proposed wood-concrete hybrid system for high-rise buildings. *Eng. Struct.* **2021**, *238*, 112194. [[CrossRef](#)]
12. Loss, C.; Pacchioli, S.; Polastri, A.; Casagrande, D.; Pozza, L.; Smith, I. Numerical Study of Alternative Seismic-Resisting Systems for CLT Buildings. *Buildings* **2018**, *8*, 162. [[CrossRef](#)]
13. Sun, X.; Li, Z.; He, M. Seismic Reliability Assessment of Mid- and High-rise Post-tensioned CLT Shear Wall Structures. *Int. J. High Rise Build.* **2020**, *9*, 175–185. [[CrossRef](#)]
14. Teweldebrhan, B.T.; Tesfamariam, S. Seismic Design of CLT Shear-Wall and Glulam Moment-Resisting Frame Coupled Structure. *J. Struct. Eng.* **2023**, *149*, 04023169. [[CrossRef](#)]
15. Hong, H.P.; Yang, S.C. Reliability and fragility assessment of the mid- and high-rise wood buildings subjected to bidirectional seismic excitation. *Eng. Struct.* **2019**, *201*, 109734. [[CrossRef](#)]
16. Dernayka, S.; Ahmed, D.; Asiz, A.; Ayadat, T.; Ajmal, M.; Holschemacher, K.; Quapp, U.; Singh, A.; Yazdani, S. Comparison of Wind Induced Response of High-Rise Buildings with Reinforced Concrete and Cross Laminated Timber. *Proc. Int. Struct. Eng. Constr.* **2022**, *9*, 21. [[CrossRef](#)]
17. Hajjaj, R.; Alhimeidi, A.; Sabbagh, M.; Alatallah, A.; Ahmed, D.; Asiz, A.; Ayadat, T.; Salman, A.; Ouda, O.K.M. Structural design and analysis of high-rise building using ultra-lightweight floor system. In Proceedings of the International Structural Engineering and Construction, Valencia, Spain, 24–29 July 2017. [[CrossRef](#)]
18. Byrick, W. Laboratory data examining impact and airborne sound attenuation in cross-laminated timber panel construction. In Proceedings of the InterNoise 2015, San Francisco, CA, USA, 9–12 August 2015.
19. Golden, M.; Byrick, W. Laboratory Data Examining Impact and Airborne Sound Attenuation in Cross-Laminated Timber Panel Construction—Part 2. In Proceedings of the InterNoise 2016, Hamburg, Germany, 21–24 August 2016.
20. Byrick, W. Laboratory impact and airborne sound attenuation in cross-laminated timber construction using resiliently mounted ceilings and poured concrete toppings. In Proceedings of the Acoustics Week in Canada, Vancouver, BC, Canada, 21–23 September 2016.
21. Ljunggren, F. Innovative solutions to improved sound insulation of CLT floors. *Dev. Built Environ.* **2023**, *13*, 100117. [[CrossRef](#)]
22. Hindman, D.P.; Golden, M.V. Acoustical Properties of Southern Pine Cross-Laminated Timber Panels. *J. Archit. Eng.* **2020**, *26*, 05020004. [[CrossRef](#)]
23. Ferik, H.; Leh, C.; Mosing, M.; Kasim, J.; Vavrik-Kirchsteiger, S.; Nusser, B. Sound.Wood.Austria—Selected measurement results of building components for multi-storey timber construction in Austria. In Proceedings of the InterNoise 2022, Glasgow, UK, 21–24 August 2022.
24. Beresford, T.; Chen, J. Floor airborne and impact sound insulation performance of cross laminated timber vs. timber joist and concrete systems. In Proceedings of the HEAR TO LISTEN—Acoustics Adelaide, Adelaide, Australia, 6–9 November 2018.
25. Hoeller, C.; Mahn, J.; Quirt, D.; Schoenwald, S.; Zeitler, B. RR-335 *Apparent Sound Insulation in Cross-Laminated Timber Buildings*; National Research Council Canada: Vancouver, BC, Canada, 2017.
26. Vardaxis, N.-G.; Bard Hagberg, D.; Dahlström, J. Evaluating Laboratory Measurements for Sound Insulation of Cross-Laminated Timber (CLT) Floors: Configurations in Lightweight Buildings. *Appl. Sci.* **2022**, *12*, 7642. [[CrossRef](#)]
27. Sabourin, I.; McCartney, C. *Measurement of Airborne Sound Insulation of 8 Wall Assemblies; Measurement of Airborne and Impact Sound Insulation of 29 Floor Assemblies*; Report No. A1-006070.10; National Research Council of Canada: Ottawa, ON, Canada, 2015.
28. Loriggiola, F.; Dall’Acqua d’Industria, L.; Granzotto, N.; Di Bella, A. Acoustics behaviour of CLT structure: Transmission loss, impact noise insulation and flanking transmission evaluations. In Proceedings of the Acoustics 2019, Cape Schanck, VIC, Australia, 10–13 November 2019.
29. Hongisto, V.; Alakoivu, R.; Virtanen, J.; Hakala, J.; Saarinen, P.; Laukka, J.; Linderholt, A.; Olsson, J.; Jarnero, K.; Keranen, J. Sound insulation dataset of 30 wooden and 8 concrete floors tested in laboratory conditions. *Data Brief* **2023**, *49*, 109393. [[CrossRef](#)]
30. Ljunggren, F. Sound insulation prediction of single and double CLT panels. In Proceedings of the 23rd International Congress on Acoustics, Aachen, Germany, 9–13 September 2019.
31. Krajči, L.; Hopkins, C.; Davy, J.L.; Tröbs, H.-M. Airborne sound transmission of a cross-laminated timber plate with orthotropic stiffness. In Proceedings of the Euronoise, Prague, Czech Republic, 10–13 June 2012.
32. Fenemore, C.; Kingan, M.J.; Mace, B.R. Application of the wave and finite element method to predict the acoustic performance of double-leaf cross-laminated timber panels. *Build. Acoust.* **2023**, *30*, 203–225. [[CrossRef](#)]
33. Dolezal, F.; Kumer, N. Simplified model for sound insulation of cross laminated timber walls with external thermal insulation composite systems. In Proceedings of the InterNoise 2019, Madrid, Spain, 16–19 June 2019.
34. Simmons, C. A systematic comparison between EN ISO 12354 calculations of CLT floors with a large set of laboratory and field measurements. In Proceedings of the EuroNoise 2021, Madeira, Portugal, 25–27 October 2021.
35. Hagberg, K.; Thorsson, P.; Golger, A.; Bard, D. SEAP—Acoustic design tool for Stora Enso Building Solutions. In Proceedings of the 22nd International Congress on Acoustics, Buenos Aires, Argentina, 5–9 September 2016.
36. Di Bella, A.; Granzotto, N.; Quartarulo, G.; Speranza, A.; Morandi, F. Analysis of airborne sound reduction index of bare CLT walls. In Proceedings of the WCTE 2018, Seoul, Republic of Korea, 20–23 August 2018.
37. Lin, J.Y.; Yang, C.T.; Tsay, Y.S. A Study on the Sound Insulation Performance of Cross-laminated Timber. *Materials* **2021**, *14*, 4144. [[CrossRef](#)]

38. Bader Eddin, M.; Ménard, S.; Bard Hagberg, D.; Kouyoumji, J.-L.; Vardaxis, N.-G. Prediction of Sound Insulation Using Artificial Neural Networks—Part I: Lightweight Wooden Floor Structures. *Acoustics* **2022**, *4*, 203–226. [[CrossRef](#)]
39. Santoni, A.; Schoenwald, S.; Van Damme, B.; Tröbs, H.-M.; Fausti, P. Average Sound Radiation Model for Orthotropic Cross Laminated Timber Plates. In Proceedings of the EuroRegio 2016, Porto, Portugal, 13–15 June 2016.
40. Santoni, A.; Schoenwald, S.; Fausti, P.; Tröbs, H.-M. Modelling the radiation efficiency of orthotropic cross-laminated timber plates with simply-supported boundaries. *Appl. Acoust.* **2019**, *143*, 112–124. [[CrossRef](#)]
41. Santoni, A. Sound Radiation and Sound Transmission in Building Structures: Numerical Modelling and Experimental Validation. Ph.D. Thesis, University of Ferrara, Ferrara, Italy, 2016.
42. Santoni, A.; Bonfiglio, P.; Fausti, P.; Schoenwald, S. Predicting sound radiation efficiency and sound transmission loss of orthotropic cross-laminated timber panels. In Proceedings of the 173rd Meeting of Acoustical Society of America and 8th Forum Acusticum, Boston, MA, USA, 25–29 June 2017. [[CrossRef](#)]
43. Yang, Y.; Fenemore, C.; Kingan, M.J.; Mace, B.R. Analysis of the vibroacoustic characteristics of cross laminated timber panels using a wave and finite element method. *J. Sound Vib.* **2021**, *494*, 115842. [[CrossRef](#)]
44. Rabold, A.; Châteauvieux-Hellwig, C.; Mecking, S.; Schramm, M. Flanking transmission of solid wood elements in multi-storey timber buildings—input data and prediction models for airborne and impact sound excitation. In Proceedings of the InterNoise 2019, Madrid, Spain, 16–19 June 2019.
45. Neusser, M.; Bednar, T. Construction details affecting flanking transmission in cross laminated timber structures for multi-story housing. In Proceedings of the InterNoise 2022, Glasgow, UK, 21–24 August 2022. [[CrossRef](#)]
46. Speranza, A.; Barbaresi, L.; Morandi, F. Experimental analysis of flanking transmission of different connection systems for CLT panels. In Proceedings of the WCTE 2016, Vienna, Austria, 22–25 August 2016.
47. Schoenwald, S.; Zeitler, B.; Sabourin, I. Analysis on Structure-borne Sound Transmission at Junctions of Solid Wood Double Walls with Continuous Floors. In Proceedings of the Forum Acusticum, Kraków, Poland, 7–12 September 2014.
48. Schoenwald, S.; Kumer, N.; Wiederin, S.; Bleicher, N.; Furrer, B. Application of elastic interlayers at junctions in massive timber buildings. In Proceedings of the 23rd International Congress on Acoustics, Aachen, Germany, 9–13 September 2019.
49. Di Bella, A.; Dall’Acqua d’Industria, L.; Valluzzi, M.R.; Pengo, A.; Barbaresi, L.; Di Nocco, F.; Morandi, F. Flanking transmission in CLT buildings: Comparison between vibration reduction index measurements for different mounting conditions. In Proceedings of the InterNoise 2019, Madrid, Spain, 16–19 June 2019.
50. Schoenwald, S.; Zeitler, B.; Sabourin, I.; King, F. Sound insulation performance of Cross Laminated Timber Building Systems. In Proceedings of the InterNoise 2013, Innsbruck, Austria, 15–18 September 2013.
51. Pérez, M.; Fuente, M. Acoustic design through predictive methods in Cross Laminated Timber (CLT) panel structures for buildings. In Proceedings of the InterNoise 2013, Innsbruck, Austria, 15–18 September 2013.
52. Guigou Carter, C.; Balanant, N.; Kouyoumji, J.-L. Acoustic Performance Investigation of a CLT-Based Three-Floor Building. *Buildings* **2023**, *13*, 213–222. [[CrossRef](#)]
53. Morandi, F.; De Cesaris, S.; Garai, M.; Barbaresi, L. Measurement of flanking transmission for the characterisation and classification of cross laminated timber junctions. *Appl. Acoust.* **2018**, *141*, 213–222. [[CrossRef](#)]
54. Mecking, S.; Kruse, T.; Schanda, U. Measurement and calculation of sound transmission across junctions of solid timber building elements. In Proceedings of the 10th European Congress and Exposition on Noise Control Engineering (EuroNoise), Maastricht, The Netherlands, 1–3 June 2015.
55. Crispin, C.; Ingelaere, B.; Van Damme, M.; Wuyts, D. The Vibration Reduction Index Kij: Laboratory Measurements for Rigid Junctions and for Junctions with Flexible Interlayers. *Build. Acoust.* **2006**, *13*, 99–111. [[CrossRef](#)]
56. Öqvist, R.; Ljunggren, F.; Ågren, A. Variations in Sound Insulation in Nominally Identical Prefabricated Lightweight Timber Constructions. *Build. Acoust.* **2010**, *17*, 91–103. [[CrossRef](#)]
57. Bard, D.; Davidsson, P.; Wernberg, P.-A. Sound and Vibrations investigations in a multi-family wooden frame building. In Proceedings of the 20th International Congress on Acoustics, Sydney, Australia, 23–27 August 2010.
58. Hörnmark, J. Acoustic Performance of Junctions in Cross Laminated Timber Constructions. Master’s Thesis, Chalmers University of Technology, Göteborg, Sweden, 2019.
59. *ISO 10848-1*; Acoustics—Laboratory and Field Measurement of Flanking Transmission for Airborne, Impact and Building Service Equipment Sound between Adjoining Rooms. Part 1: Frame Document. International Organization for Standardization: Geneva, Switzerland, 2019.
60. Nilsson, E.; Ménard, S.; Bard, D.; Hagberg, K. Effects of building height on the sound transmission in cross-laminated timber buildings—Airborne sound insulation. *Build. Environ.* **2023**, *229*, 109985. [[CrossRef](#)]
61. Murta, B.; Höller, C.; Sabourin, I.; Zeitler, B. Measurement of structural reverberation times for calculation of ASTC in upcoming NBCC. In Proceedings of the Acoustic Week in Canada 2014, Winnipeg, MB, Canada, 8–10 October 2014. [[CrossRef](#)]
62. Bietz, H.; Wittstock, V. Comparison of Different Methods for the Determination of Structure-Borne Noise Reverberation Time. In Proceedings of the CFA-DAGA’04, Strasbourg, France, 22–25 March 2004.
63. Nilsson, E.; Ménard, S.; Hagberg, D.B.; Hagberg, K. Effect of Bearing Direction and Mounting Techniques on Cross-Laminated Timber Elements in the Field. In Proceedings of the InterNoise 2022, Glasgow, UK, 21–24 August 2022. [[CrossRef](#)]
64. *ISO 3382-2*; Acoustics—Measurement of Room Acoustic Parameters. Part 2: Reverberation Time in Ordinary Rooms. International Organization for Standardization: Geneva, Switzerland, 2008.

65. Hopkins, C.; Robinson, M. On the Evaluation of Decay Curves to Determine Structural Reverberation Times for Building Elements. *Acta Acust. United Acust.* **2013**, *99*, 226–244. [[CrossRef](#)]
66. Pontius, R.G.; Thontteh, O.; Chen, H. Components of information for multiple resolution comparison between maps that share a real variable. *Environ. Ecol. Stat.* **2007**, *15*, 111–142. [[CrossRef](#)]
67. Hopkins, C. *Sound Insulation*, 1st ed.; Routledge: London, UK, 2007.

**Disclaimer/Publisher’s Note:** The statements, opinions and data contained in all publications are solely those of the individual author(s) and contributor(s) and not of MDPI and/or the editor(s). MDPI and/or the editor(s) disclaim responsibility for any injury to people or property resulting from any ideas, methods, instructions or products referred to in the content.